

# Magnetic Omnidirectional Wheels for Climbing Robots

Mahmoud Tavakoli<sup>1</sup>, Carlos Viegas<sup>1</sup>, Lino Marques<sup>1</sup>, J. Norberto Pires<sup>2</sup> and Aníbal T. de Almeida<sup>1</sup>

**Abstract**—This paper describes design and development of omnidirectional magnetic climbing robots with high maneuverability for inspection of ferromagnetic 3D human made structures. The main focus of this article is design, analysis and implementation of magnetic omnidirectional wheels for climbing robots. We discuss the effect of the associated problems of such wheels, e.g. vibration, on climbing robots. This paper also describes the evolution of magnetic omnidirectional wheels throughout the design and development of several solutions, resulting in lighter and smaller wheels which have less vibration and adapt better to smaller radius structures. These wheels are installed on a chassis which adapts passively to flat and curved structures, enabling the robot to climb and navigate on such structures.

## I. INTRODUCTION

Climbing robots have been developed during the past two decades in order to facilitate some jobs such as periodical inspections for detection of cracks, corrosion, material degradation and welding defects on tanks and piping. Other applications of interest include ship hull grooming, cleaning, and painting of such structures. Gas and oil tanks, Wind turbines, pipelines and marine vessels are examples of the structures which are target of this research work. Such structures share three common aspects:

- They need periodic inspection, maintenance or cleaning
- Their exterior circumference is convex
- Most of them are built from ferromagnetic material

For climbing a surface, design of the locomotion mechanism and the surface adherence mechanism are the main challenges. Excluding the biological imitation adherence mechanisms, adherence systems developed up to now are based on suction cups (See for instance [1], [2]), attraction force generated by propeller (negative pressure) [3], [4] or magnets [5], [6]. Robots whose end-effectors match engineered features of the environment like fences or porous materials, pipes or bars [7], [8], [9], [10], [11], [12] were also developed.

As the desired structures for this project are ferromagnetic, and not always flat, usage of negative pressure is not the best choice due to the energy consumption and curvature adaptability problems. In such situations, magnetic adherence is a more appropriate choice. Some of the applications e.g. painting or cleaning or periodical inspection need the robot be able to scan the whole structure or to reach to a pose on the structure rapidly and then perform in situ maintenance

(welding, repairing, etc.). In both cases high navigation velocity is desirable.

Furthermore, in all cases high maneuverability is desired. One of the most important limitations of many pole climbing robots is that they can not rotate around the pole [13], or in order to rotate around the pole, they have high energy and time costs [14], [15], [16], while rotating around the pole is necessary for being able to scan the whole structure. Another important aspect is adaptability of the robot to various structures.

The main objective of this research is to implement a robot which is able to climb and navigate over ferromagnetic structures considering:

- High maneuverability.
- High speed.
- Adaptability to a reasonable range of curvature.
- Adaptability to a reasonable range of structure's ferromagnetic materials and thickness.
- Simplicity.

Climbing robots based on permanent magnets have also been developed for different purposes. They were based on a magnetic caterpillar[17], magnetic array wheel [18] or permanent magnetic wheels [6]. Yet there is a lot of space for improvements on many aspects of magnetic wheel based climbing robots. In the current research we tried to concentrate on aspects of climbing robots such as maneuverability and adaptability to various structures. The first version of the omnidirectional climbing robot, the OmniClimber-I, was introduced in [19]. Results from OmniClimber-I showed a good maneuverability and adaptability to several structures. However due to the discontinuous movement nature of omnidirectional wheels, the robot could not achieve a smooth movement. We will discuss how a climbing robot based on omnidirectional wheels suffers more from a chattering in movement than a terrestrial robot, and will try to improve such problem. Some other parameters such as size and weight of the wheel, normal attraction force, friction coefficient and adaptability to curved structures were also considered and novel designs of the wheel were implemented. Some improvements on central and side magnets were also achieved. The results obtained and improvements achieved to the overall performance of the robot are described in this paper.

## II. OMNICLIMBER CONCEPT

In design of OmniClimbers we try to address maneuverability on the structure and adaptability to different structures. Here we shortly describe the Omniclimbers concept.

<sup>1</sup>Institute for Systems and Robotics, Dep. of Electrical and Computer Eng., University of Coimbra, Portugal. {mahmoud, carlosviegas, lino, adealmeida}@isr.uc.pt<sup>2</sup>Dep. of Mechanical Eng., University of Coimbra norberto@dem.uc.pt

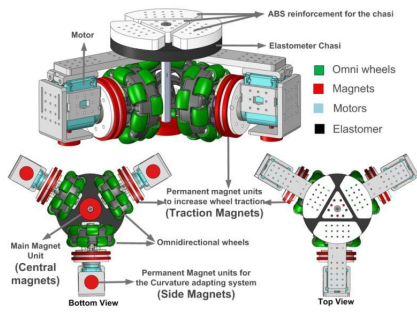


Fig. 1. Omniclimber-I is composed of a central magnet unit, a flexible chassis and side magnets, and omnidirectional wheels coupled with ring magnets

More detailed description can be found in [20]. OmniClimbers involve the following main novelties (figure 1 shows the 3D model of OmniClimber-I):

- 1) **Utilizing omnidirectional wheels in order to increase maneuverability**
- 2) **Flexible chassis with side magnets for non-actuated adaptation to the curvature:** We used an elastomer in the chassis and integrated permanent magnets in order to enable the robot to adapt to a range of curvatures with a simple non actuated (passive) system (figure 1).

As described in [19] omniClimber-I is a 3-DOF robot composed of 3 rotational actuators and 3 Omnidirectional wheels placed at  $120^\circ$ . It also includes a central magnet to hold the robot attached to the climbing surface, side magnets and a flexible chassis for curvature adapting system and ring magnets installed close to the wheels in order to increase the wheel traction (figure 1).

### III. OMNIDIRECTIONAL WHEELS FOR CLIMBING ROBOTS

Omnidirectional wheels form the most important part of the omniclimbers which enables high maneuverabilities. However they have some disadvantages such as vibration. It is important to consider the effect of vibration on terrestrial robots using omnidirectional wheels and analyze how vibration affects a climbing robot with such wheels. Figure 2 [21] shows various types of omnidirectional wheels.

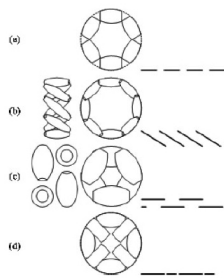


Fig. 2. Various types of Omnidirectional wheels and their traces; (a) Classic 1 row omniwheel, (b) Mecanum, (c) Classic 2 rows omniwheel, (d) continuous alternate wheel [21].

As discussed in [21], the classic type of omnidirectional wheels (figure 2-a) makes discontinuous contacts with the

ground due to the gaps between the successive rollers, which causes vertical vibration. To minimize this gap, Mecanum wheels, double row wheels, alternate wheels and half wheels were developed. In none of these wheels the gap is totally removed. In our case we used double row wheels which has a better coverage relative to the classic wheels and is also simple to develop with standard elements and commercially available magnetic rings. Yet double row wheels suffer also from horizontal vibrations. Small vibrations may not be a problem in terrestrial robots, but in case of climbing robots, such vibration affects the normal adhesive force. In case of omniclimbers, horizontal vibrations on the chassis affect the normal magnetic force of the side magnets and traction magnets, considering that the climbing structure is not flat and horizontal movements change the distance of the magnets with the structure. The magnetic force has an inverse relation with the cubic order of the distance from surface (see equation 1). Therefore as we experienced with OmniClimber-I, small vibrations changes the normal magnetic force on each wheel which causes undesired vibrations in the direction normal to the surface and thus results in a non smooth movement. Furthermore a difference on normal magnetic force causes a difference on each wheel's traction, resulting in a low trajectory following accuracy. To manage such vibrations, the normal force is a critical aspect. Higher normal forces reduces vertical vibrations. In omniclimber-I we calculated normal forces generated from side magnets and traction magnets in such a way that not only they guarantee adherence to the surface in static and dynamics modes but also they establish enough traction on the wheels. But to reduce the vibrations, normal forces should be higher than the calculated values in Omniclimber-I, so that the traction is guaranteed even in case of existence of vibrations and that such vibration could not detach the wheel from the structure. However excessive magnetic force requires bigger and heavier magnets, and results in higher torque requirements, and thus the goal is to find the right balance between magnetic force and weight on the wheels. We also tried to improve other important aspects of omnidirectional wheels for climbing robots, such as weight, size, adaptation to curved structures and traction. In any climbing robot, the weight is a crucial aspect. All components of the robot should be lightweight, including the wheels. The size of the magnetic omnidirectional wheel is also a key aspect. Smaller wheels result in reduction of the weight of the whole robot and the bending forces to the chassis. Reducing the size of the wheels contributes to a higher driving force at the same motor driving torque, but also a reduction on the climbing speed. Four versions of omnidirectional wheels with magnetic adherence were designed, developed and tested, and the results are reported in this paper.

### IV. DESIGN AND DEVELOPMENT OF MAGNETIC OMNIDIRECTIONAL WHEELS

In this section we present the design, analysis and development of the wheels, their testing, results and problems observed. The fourth generation of the magnetic omnidirec-

tional wheel is the result of all the studies and lessons taken and learned with the previous solutions.

### A. 1<sup>st</sup> Generation

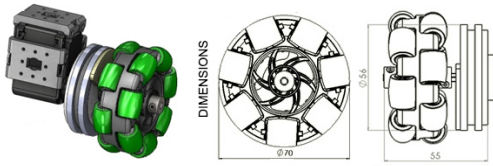


Fig. 3. Design of the 1<sup>st</sup> generation of magnetic wheels.

The first generation wheel, used in Omniclimber-I, was 70 mm diameter, 55 mm width and 150g of mass (figure 3). It used a ring magnet as the traction magnet. In order to avoid the direct contact between the magnetic rings and the surface, a high distance between the ring magnet and the surface was necessary (figure 4). However, such distance prevented the magnets from providing significant force, especially in thin metallic surfaces.

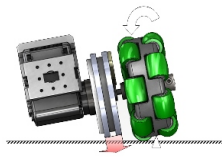


Fig. 4. To avoid direct contact of the magnet with the surface and tilting of the wheel, the ring magnet should be small enough to keep a certain distance from the surface, which reduces the normal magnetic force.

### B. 2<sup>nd</sup> Generation

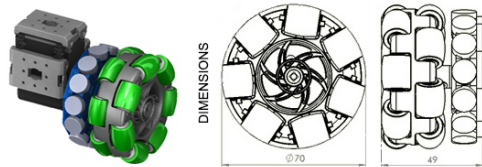


Fig. 5. Design of the 2<sup>nd</sup> generation of magnetic wheels, with adjustable distance between the magnets and the surface.

The second generation of the OmniClimber wheel offered some improvements on the adjustability of the system. It consisted on an array of individual magnets, where the distance between the magnets and the surface could vary, by means of manual adjustment (figure 5). This improved the wheel adherence and traction to thin metallic surfaces. The problem was that they did not provide a continuous magnetic adhesion. To select the number of magnets in an array (figure 6), we analyzed the magnetic force of the wheel with 6 to 16 magnets, comparing dimensions, mass, minimum and maximum magnetic force and its variation and prototyping limitations (graph 7 and table I).

The maximum magnetic attraction force occurs when one of the magnets is parallel to the surface and minimum

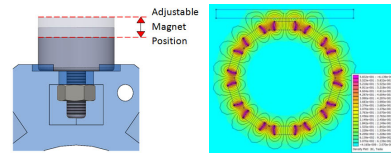


Fig. 6. On the left: Adjustable Magnet Positioning System. On the right: 2D Magnetic Flux Field Representation.

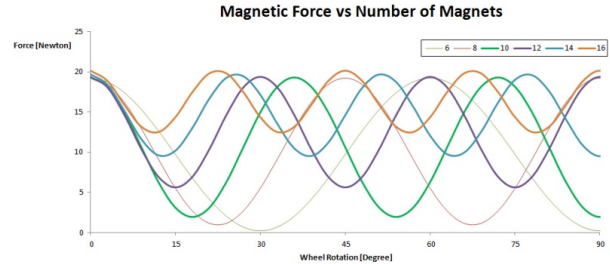


Fig. 7. Magnetic Force Analytically determined for each solution, for 90°degree rotation of the wheel.

attraction force occurs when all magnets are tilted relative to the surface (figure 8). Magnetic force for each solution was estimated, considering the influence of the number of magnets, the tilt of each magnet on the wheel ( $\alpha$ ) and its distance to the surface ( $d$ ), illustrated on the figure 9. The influence of the tilt of a permanent magnet on its force was determined by magnetic field simulation software (figure 10).

We used the following equation for estimating the attraction force at certain distance, based on the attraction force on zero distance, according to the HKCM website[22]:

$$F_r = \frac{F_h}{1 + s^3} \quad (1)$$

Where  $F_r$  is the attraction force at the distance of  $s$ , and  $F_h$  is the attraction force at the distance of zero. This equation provides an estimate and not a precise value. With the knowledge of the magnet's distance to surface and tilt we were able to calculate the attraction force for each array. The best trade off was achieved with a wheel with array of 14 cylindrical magnets with 12 mm in diameter and adjustable distance to surface (table I). As can be seen in figure 12, for lower number of magnets, e.g. 6 magnets, the maximum

Number of Magnets	6	8	10	12	14	16
Wheel mass [g]	125	135	145	155	165	175
Min Force [N]	0.20	0.97	1.90	5.61	9.50	12.43
Max Force [N]	19.19	19.20	19.26	19.39	19.66	20.13
Average Force [N]	9.69	10.08	10.58	12.50	14.58	16.28
Average force relative to array of 6	1.00	1.04	1.09	1.29	1.50	1.68

TABLE I

PERFORMANCE TABLE FOR EACH SOLUTION, REGARDING 90°DEGREES OF WHEEL ROTATION.

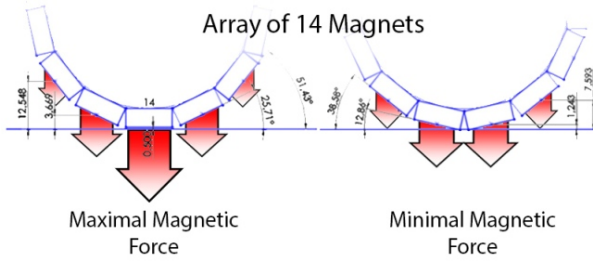


Fig. 8. Wheel positions for maximal and minimal magnetic force. The maximum magnetic attraction force occurs when one of the magnets is parallel to the surface and the minimum attraction force occurs when all magnets are tilted relatively to the surface.

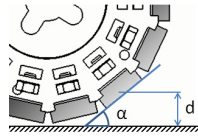


Fig. 9. For each wheel with an array of magnets from 6 to 16, we calculated the magnetic force for the closest magnets to the surface, taking into account its distance and angle.

magnetic force (19.19 N) is almost 100 times bigger than the minimum magnetic force (0.20 N). In a solution with 14 magnets this ratio is as low as 2. The 16 magnets wheel proved to be impractical to be prototyped due to the size restrictions. Giving the adjustment possibility to the new wheel, the tilting problem (figure 11) was reduced for curved structures, which allows a closer distance between magnets and the surface and a higher attraction force on the wheel. This wheel is 70 mm in diameter and 49 mm in width, and has a mass of 165 g. Yet the tilting problem was not completely addressed. To address this problem, we decided to put the traction magnets in the center (and not in the side) of the omnidirectional wheel.

### C. 3<sup>rd</sup> Generation

This third generation of the omni-wheel integrates the magnetic array into the omnidirectional wheel, resulting in reduction of the overall size of the system. Similar to the

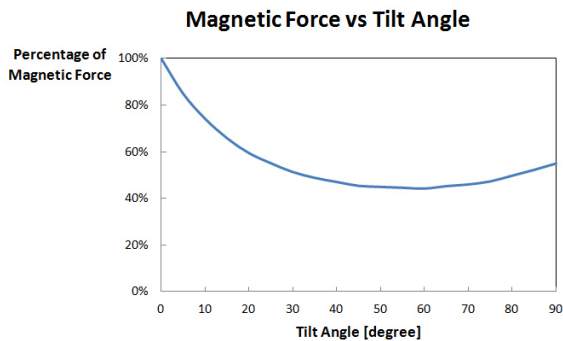


Fig. 10. Influence of the tilt of the magnet on the magnetic force to a fixed ferromagnetic structure, determined by magnetic field simulation software. The force increase after 45° is due to summation of attraction force from two sides of the permanent magnet.

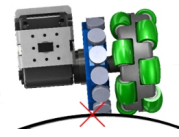


Fig. 11. The normal force of the 2<sup>nd</sup> generation of the wheel is 2.45 times of the first generation, however the tilting problem is not yet solved.

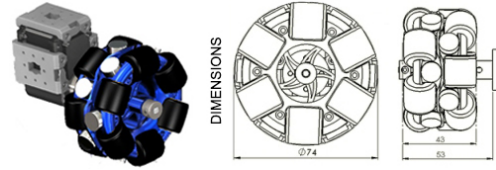


Fig. 12. 3<sup>rd</sup> generation of magnetic omnidirectional wheels.

second generation, the distance between the magnets and the surface are adjustable. Placing the magnet array between the rollers, eliminated the tilting problem of the wheel in the previous two generations. Therefore magnets could be placed at a distance very near to the surface, thus providing a bigger adherence force and a better traction compared to the previous solutions. Thus we were able to reduce the number of magnets to 12. Yet the resulting wheel has a mass of 185 gr, which means it is slightly heavier than the previous solution only because we had to develop the whole wheel rather than using commercial wheels.

Our experiments showed this wheel represented major improvements compared to the previous generation in terms of motion smoothness and trajectory following, since it suffered from less vibration. Yet with this design, the roller coverage was not perfect (-5.73° gap between the rollers as shown in picture 13), which causes some vibrations. The other problem is that the wheel is too wide, which is not desired for curved structures and relatively heavy (74 mm in diameter, 43 mm in width, 185g of mass, see picture 12).

### D. 4<sup>th</sup> Generation and current development

From the three previous developments, and several tests, we concluded that the magnet adherence elements for wheel

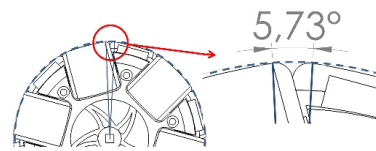


Fig. 13. Gap of the roller coverage in the 3<sup>rd</sup> generation of the magnetic omni-wheel.



Fig. 14. Design of the 4<sup>th</sup> generation of magnetic wheels.

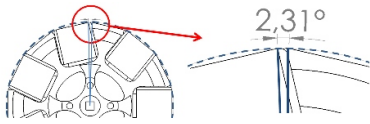


Fig. 15. Roller coverage of the 4<sup>th</sup> generation of magnetic wheels.

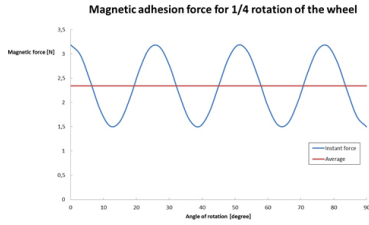


Fig. 16. Magnetic force for the 4<sup>th</sup> generation of the magnetic wheel for a 90°degrees rotation.

tracking should be placed on the wheel itself rather than on its side. We also concluded that in climbing robots, vibration resulting from omnidirectional wheels reduces the robot trajectory following accuracy and may totally impair the climbing process. It is important to reduce the vibration effect as much as possible. Therefore we considered the previous factors, and simultaneously we tried to reduce the wheels' size and weight. In The fourth generation (figure 14), we integrated magnetic rollers, resulting in a much smaller and lighter solution (65 mm in diameter and 30 mm in width, 105 g of mass, representing 12%, 30% and 43% reduction compared to the previous generations, respectively). Each roller is composed of two ring magnets with same polarities facing each other. In this way the magnetic flux and thus the magnetic force is increased by 30% (Simulated by magnetic field simulation software and also verified experimentally). We achieved the optimal solution by an array of 14 magnetic rollers disposed in two rows. This design allows for a better coverage and less gap between the rollers (2.31°, compared to 5.73°in the previous design as can be seen in figure 15) and thus there exist less vibration. The magnetic adherence provided by the wheel during its rotation was calculated using the same method described before. The values achieved for the magnetic forces are inferior to the ones in previous designs. However, since we are dealing with a lighter and smaller wheel, the required magnetic adhesion forces is also smaller (figure 16). The smaller wheel size allows for a smaller chassis, resulting in a lighter solution and a more compact robot design. Nickel coated magnets, have a low friction coefficient on steel and the friction coefficient should be increased for a better traction, and thus it was necessary to cover them with a high friction material. On the other hand this cover would reduce the normal magnetic force and thus a trade off should be achieved. We tested the magnetic rollers in three cases: without cover, with a 0.4 mm thick thermal shrink layer, and with a 1 mm thick silicone rubber tire (we tested the commercially available solutions). We performed two tests (see figure 17) in order to measure the normal force and also the coefficient of friction  $\mu$ . In the first experiment

we determined the magnetic force,  $F_m$ , for each solution by measuring the required force to detach the assembly from the vertical steel wall.

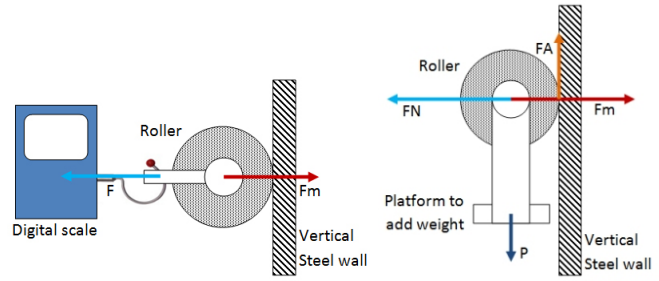


Fig. 17. Assembly of the 1<sup>st</sup> (Left) and 2<sup>nd</sup> (right) experiments for measuring the normal force and coefficient of friction of the rollers

In the second experiment, the roller rotation was restricted so that it can only slide. This allows us to evaluate the static friction coefficient for each tire solution. This is when the weight (P) of the assembly is equal to the friction force  $F_A$ . Therefore we determined the friction coefficient for each solution:

$$\begin{cases} FA = P \\ FN = Fm \end{cases}$$

$$\mu FN = mg \rightarrow \mu = \frac{mg}{Fm}$$

As can be seen in table II, even though the magnetic adherence of the roller with silicone tire was inferior to the one with the thermal shrink tire (-25%), its performance was better in providing grip for the wheels (+84%). The product between the static friction coefficient and the magnetic force for each solution is maximum for the silicone layer (II) and thus we used the silicon tube cover for the rollers. So that

Type of Roller	Layer thickness(mm)	Magnetic force(N)	Mass held (g)	$\mu_{static}$	$\mu \times Fm$
No cover layer	0	3.09	50	0.16	0.49
Thermal shrink layer	0.4	1.91	92	0.50	0.96
Silicone layer	1	1.42	134	0.92	1.31

TABLE II  
RESULTS OF THE ROLLER EXPERIENCES.

was the solution adopted for the rollers.

After all the best  $\mu_f \cdot F_N$  value was achieved by placing two ring magnets with same poles facing each other, and covering the assembly by a silicon tube. Figure 14 shows dimensions of the 4<sup>th</sup> generation of the wheel.

### E. Comparison

Table III compares the characteristics of all four generations. A key factor for the comparison is the normal magnetic attraction force to weight ratio for all solutions. As can be seen in the table, this value is increased through evolution of the wheels. Another important factor is how well the double row wheels adapt to a curved surface. While the first two generations suffer from the tilting problem, this

Parameters				
Wheel mass [g]	150	165	185	105
Size (Diam x Width) [mm]	70 x 55	70 x 49	74 x 43	65 x 30
Normal Force [N]	0.80	1.97	4.49	3.20
Normal Force/Weight ratio [N/g]	0.005	0.012	0.024	0.030
Double row adaptation to curvature	*	*	**	***

TABLE III  
COMPARISON BETWEEN THE DEVELOPED SOLUTIONS.

is solved in the third generation, and thus both rows of wheels have effective contact with the surface. In the fourth generation, the coverage of the rollers was increased and thus the vibration was decreased, allowing for a smoother movement. Also the size and the weight of the wheel was reduced, resulting in a smaller robot.

#### VIDEO ATTACHMENT

This article is accompanied by a video showing the experiments of the Omniclembers on flat and curved structures.

#### V. CONCLUSIONS AND FUTURE WORKS

In this paper we presented evolution of omnidirectional magnetic wheels, which resulted in a lighter and smaller wheels which suffers from less vibration, and adapt better to curved structures. Future works includes development of a fully round omnidirectional magnetic wheels and integration of exteroceptive sensors to compensate the odometry errors, and a vision system for inspection of the structure.

#### VI. ACKNOWLEDGMENT

This research work was partially supported by the Portuguese Foundation of Science and Technology, SFRH/BPD/70557/2010 & PTDC/EME-CRO/121547/2010.

#### REFERENCES

- [1] D. Longo and G. Muscato, "A modular approach for the design of the alicia climbing robot for industrial inspection," *Industrial Robot: An International Journal*, vol. 31, no. 2, pp. 148–158, 2004.
- [2] Z. Qian, Y. Zhao, and Z. Fu, "Development of wall-climbing robots with sliding suction cups," in *IEEE/RSJ International Conference on Intelligent Robots and Systems*. IEEE, 2006, pp. 3417–3422.
- [3] A. Nishi, "A wall climbing robot using propulsive force of propeller," in *Proc. IEEE Int. Conf. on Advanced Robotics, ICAR*, 1991, pp. 320–325.
- [4] J. Xiao, W. Morris, N. Chakravarthy, and A. Calle, "City climber: a new generation of mobile robot with wall-climbing capability," in *Proceedings of SPIE*, vol. 6230, no. 1, 2006.
- [5] S. Hirose, A. Nagabuko, and R. Toyama, "Machine that can walk and climb on floors, walls, and ceilings," in *Proc. IEEE Int. Conf. on Advanced Robotics*, Pisa, Italy, June 1991, pp. 753–758.
- [6] F. Tâche, W. Fischer, R. Siegwart, R. Moser, and F. Mondada, "Compact magnetic wheeled robot with high mobility for inspecting complex shaped pipe structures," in *Intelligent Robots and Systems, 2007. IROS 2007. IEEE/RSJ International Conference on*. IEEE, 2007, pp. 261–266.
- [7] M. Tavakoli, L. Marques, and A. de Almeida, "Self calibration of step-by-step based climbing robots," in *IEEE/RSJ International Conference on Intelligent Robots and Systems*. IROS, 2009, pp. 3297–3303.
- [8] —, "A low cost method for self calibration of pole climbing robots," *Robotica*, 2010.
- [9] C. Balaguer, A. Giménez, J. Pastor, V. Padrón, and M. Abderrahim, "A climbing autonomous robot for inspection applications in 3D complex environments," *Robotica*, vol. 18, no. 03, pp. 287–297, 2000.
- [10] M. Almonacid, R. Saltaren, R. Aracil, and O. Reinoso, "Motion planning of a climbing parallel robot," *IEEE Transactions on Robotics and Automation*, vol. 19, no. 3, pp. 485–489, 2003.
- [11] M. Tavakoli, M. Zakerzadeh, G. Vossoughi, and S. Bagheri, "A hybrid pole climbing and manipulating robot with minimum DOFs for construction and service applications," *Journal of Industrial Robot*, vol. 32, no. 2, pp. 171–178, March 2005.
- [12] M. Tavakoli, L. Marques, and A. de Almeida, "3DCLIMBER: Climbing and manipulation over 3D structures," *Journal of Mechatronics*, vol. 21, no. 1, pp. 48–62, 2011.
- [13] C. Balaguer, J. Pastor, A. Giménez, V. Padrón, and M. Abderrahim, "Roma: A multifunctional autonomous self-supported climbing robot for inspection application," in *3rd IFAC Symposium on Intelligent Autonomous Vehicles*, Madrid, Spain, 1998, pp. 357–362.
- [14] J. Sabater, R. Saltarén, R. Aracil, E. Yime, and J. Azorin, "Teleoperated parallel climbing robots in nuclear installations," *Industrial Robot: An International Journal*, vol. 33, no. 5, pp. 381–386, 2006.
- [15] M. Tavakoli, L. Marques, and A. de Almeida, "Development of an industrial pipeline inspection robot," *Industrial Robot: An International Journal*, vol. 37, no. 3, pp. 309–322, 2010.
- [16] M. Tavakoli, G. Cabrita, R. Faria, L. Marques, and A. T. de Almeida, "Cooperative multi-agent mapping of three-dimensional structures for pipeline inspection applications," *The International Journal of Robotics Research*, vol. 31, no. 12, pp. 1489–1503, 2012.
- [17] P. Schoeneich, F. Rochat, O. T.-D. Nguyen, R. Moser, and F. Mondada, "Tripillar: a miniature magnetic caterpillar climbing robot with plane transition ability," *Robotica*, vol. 29, no. 7, pp. 1075–1081, 2011.
- [18] M. Eich and T. Vogele, "Design and control of a lightweight magnetic climbing robot for vessel inspection," in *Control & Automation (MED), 2011 19th Mediterranean Conference on*. IEEE, 2011, pp. 1200–1205.
- [19] M. Tavakoli, L. Marques, and A. de Almeida, "Omniclember: An omnidirectional light weight climbing robot with flexibility to adapt to non-flat surfaces," in *IEEE/RSJ International Conference on Intelligent Robots and Systems (IROS)*. IEEE, 2012.
- [20] M. Tavakoli, C. Viegas, L. Marques, J. N. Pires, and A. T. de Almeida, "Omniclembers: Omni-directional magnetic wheeled climbing robots for inspection of ferromagnetic structures," *Robotics and Autonomous Systems*, vol. 61, no. 9, pp. 997 – 1007, 2013. [Online]. Available: <http://www.sciencedirect.com/science/article/pii/S0921889013001024>
- [21] K.-S. Byun and J.-B. Song, "Design and construction of continuous alternate wheels for an omnidirectional mobile robot," *Journal of Robotic Systems*, vol. 20, no. 9, pp. 569–579, 2003.
- [22] P. magnet distributor, "<http://www.hkcm.de>," Web reference, Jan 2012.